



Open Access : : ISSN 1847-9286

www.jESE-online.org

Original scientific paper

Effect of heat treatment on structure and properties of multilayer Zn-Ni alloy coatings

VAISHAKA R. RAO, A. CHITHARANJAN HEGDE[✉] and K. UDAYA BHAT*

Electrochemistry Research Laboratory, Department of Chemistry, National Institute of Technology Karnataka, Surathkal, Srinivasnagar-575025, India

**Department of Metallurgy and Materials Engineering, National Institute of Technology Karnataka, Surathkal, Srinivasnagar-575025, India*

[✉]Corresponding Author: E-mail: hegdeac@rediffmail.com, Tel.: +91-9980360242

Received: December 25, 2012; Revised: April 12, 2013; Published: November 09, 2013

Abstract

Composition modulated multilayer alloy (CMMA) coatings of Zn-Ni were electrodeposited galvanostatically on mild steel (MS) for enhanced corrosion protection using single bath technique. Successive layers of Zn-Ni alloys, having alternately different composition were obtained in nanometer scale by making the cathode current to cycle between two values, called cyclic cathode current densities (CCCD's). The coatings configuration, in terms of compositions and thicknesses were optimized, and their corrosion performances were evaluated in 5 % NaCl by electrochemical methods. The corrosion rates (CR)'s of multilayer alloy coatings were found to decrease drastically (35 times) with increase in number of layers (only up to 300 layers), compared to monolayer alloy deposited from the same bath. Surface study was carried with SEM, while XRD was used to determine metal lattice parameters, texture and phase composition of the coatings. The effect of heat treatment on surface morphology, thickness, hardness and corrosion behaviour of multilayer Zn-Ni alloy coatings were studied. The significant structural modification due to heat treatment is not accompanied by any decrease in corrosion rate. This effect is related to the formation of a less disordered lattice for multilayer Zn-Ni alloy coatings.

Keywords

Multilayer Zn-Ni alloy; Corrosion study; Heat treatment; SEM; XRD.

Introduction

An advanced coating technique, called composition modulated multilayer alloy (CMMA) coating is gaining interest due to their improved properties, such as mechanical strength/hardness, enhanced diffusivity, improved ductility/toughness, reduced density, reduced elastic modulus, increased specific heat, higher thermal expansion coefficient, lower thermal conductivity, enhanced corrosion

and wear resistance, superior reflectance, soft magnetic properties, giant magnetoresistance and corrosion resistance not attainable in any of the metallurgical alloys [1]. The CMMA materials basically consists of alternating layers of metals/alloys on micro/nanometer scale, deposited electrolytically by making the cathode to cycle between two current densities at definite time intervals. The coating with improved resistance to highly aggressive environmental condition is demanded for the extended safe service life of industrial objects. Hence CMMA coating is well studied while finding its wide spread industrial applications [2-4].

Blum first introduced the electrodeposition of multilayered alloy on Cu-Ni, demonstrating the deposition of alternate Cu and Ni layers, tens of microns thick, from two different electrolytes [5]. The deposition using Single Bath Technique (SBT) for the fabrication of modulated alloys was recorded by Brenner [6]. Tench and White proposed that the presence of Ni in the deposit was responsible for improved corrosion resistance of fabricated Cu/Ni metal multilayers and also their mechanical properties [7]. The Zn-Ni alloy electrodeposition has attracted interest of scientific community because these alloys were found to be more corrosion resistant and thermally stable than pure zinc [8]. Many authors have attempted to understand the characteristics of this deposition process [9-12]. The abrupt change in the composition of the alloys and in the current efficiency is observed during this complex codeposition at a given value of deposition potential/current density. Multilayer coating by electrolytic method is the most promising approach for improving the corrosion resistance of Zn-Ni alloys, and is of distinct commercial interest [13-16]. The CMMA coating with Zn-Fe alloy as alternate layers was tested to exhibit better corrosion protection than individual metals. The presence of high content of Fe in Zn-Fe alloy was reasoned to be responsible for enhanced corrosion protection [17].

The thermal stability of the Zn-Ni alloy coatings is important for their general applications, especially where they are expected to perform at elevated temperature conditions, such as in some automotive applications. However, the conventional methods usually modify the physical properties of the metal being protected with the limitations, such as susceptibility to damage by heat, cost, and formation of oxide products. The real challenge to overcome these problem would be to develop a novel protection coating with an exceptional thermal stability with minimum changes to the physical properties of the protected metal. Though there are many reports with regard to the development of CMMA Zn-Ni coatings using different baths and additives, no work has been reported with regard to examine the thermal stability of those coatings [18-21]. Hence the present paper reports the development of CMMA Zn-Ni alloy coatings on mild steel (MS) from acid chloride bath using gelatin and glycerol as additives. The corrosion stability of CMMA Zn-Ni coatings on heat treatment have been tested by subjecting the coated specimens to different temperatures. The CMMA Zn-Ni coatings have been tested for their thickness, hardness, composition, surface morphology and corrosion stability before and after heat treatment, and results are discussed.

Experimental

All electrodeposition were carried out from the same electrolytic bath prepared using analytical grade reagents and double distilled water. Conventional Hull cell method was used to examine the effect of current density (c.d.) and bath constituents [22]. The Zn-Ni alloy bath was prepared by adding known amount of gelatin in hot distilled water (insoluble in cold water) and glycerol as additives, to impart brightness to the coating. Electroplating process was carried out in a stirred solution on a pre-cleaned MS panels, having 7.5 cm^2 active surface area, at $30 \text{ }^\circ\text{C}$ and pH 4.0. The Zn anode was used with the same exposed area. The electroplating of both monolayer (mono-

lithic) and CMMA Zn-Ni coating was carried out using computer controlled DC power source, having output speeds of up to 160 microseconds per step voltage/current change (N6705A, Agilent Technologies) for 10 min ($\sim 15 \mu\text{m}$ thickness), for comparison purpose. The coating thickness were determined by Faraday's law and verified by measuring in Digital Thickness Meter (Coatmeasure - M&C, AA Industries/Yuyutsu Instruments). The hardness of coatings was measured using Digital Micro Hardness Tester (CLEMEX, Model: MMT-X7). The electrodeposited MS plates were subjected to heat treatment by keeping in temperature controlled oven (Technico Ind. Ltd., 3144) at temperature 100, 200, 300 and 400 °C for constant time duration of 60 minutes. The modulation in the composition of alternate layer was affected by pulsing the current periodically. The power pattern used for deposition of monolayer (direct Current) and multilayer (pulsed current) coatings is shown in Figure 1. The optimal composition and operating parameters of the bath is given in Table 1.

The corrosion behavior of the coatings were evaluated in 5 % NaCl solution at pH 4.0 using Potentiostat/Galvanostat (ACM Instruments, Gill AC Series No-1480) at temperature 25 °C, using saturated calomel electrode (SCE) as reference, and platinum as counter electrodes, respectively. The corrosion rates (CR) were measured by Tafel extrapolation method at scan rate of 1 mV s^{-1} with start potential +250 mV to reverse potential -500 mV. The electrochemical impedance spectroscopy (EIS) measurements were made in frequency range of 100 kHz to 0.01 Hz at $\pm 10 \text{ mV}$ perturbing voltage, to evaluate the barrier property of the coatings. The surface morphology and cross sectional view of the CMMA coating were examined under Scanning Electron Microscopy (SEM, Model JSM-6380 LA from JEOL, Japan). The variation in the phase structure of alloys in different layers were confirmed by X-ray diffraction (XRD) study, using Cu $K\alpha$ ($\lambda = 0.15405 \text{ nm}$) radiation, in continuous scan mode with a scan rate of 2° min^{-1} (XRD, JEOL JDX-8P). Conveniently, Zn-Ni CMMA coatings are represented as: $(\text{Zn-Ni})_{1/2/n}$ (where 1 and 2 indicate the first and second cathode current density (CCCD's) and 'n' represent the number of layers formed during total plating time. *i.e.* 10 min.

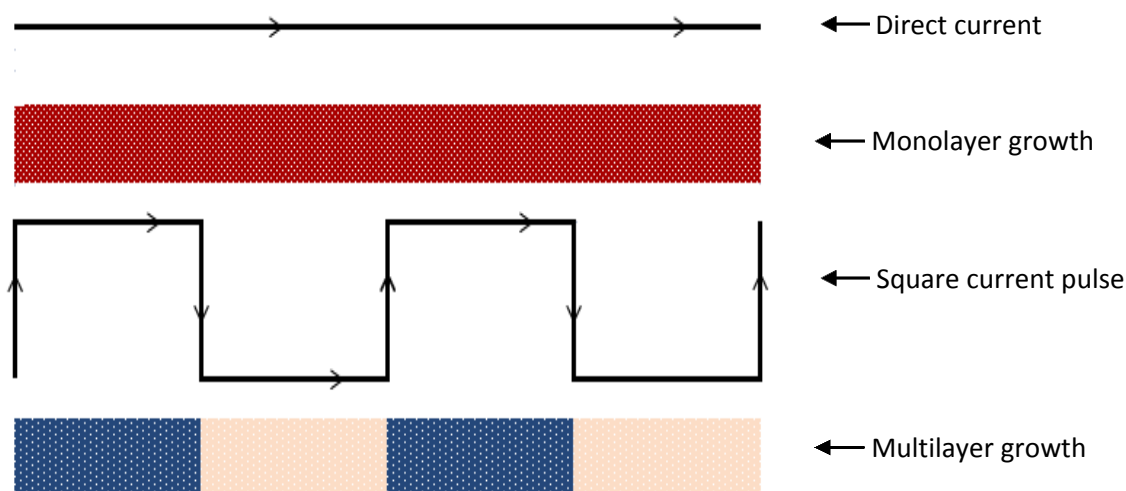


Figure 1. Power pattern used for deposition of monolayer (direct current) and multilayer (square current pulse) coatings.

Results and Discussion

Monolayer Zn-Ni alloy coatings

The Hull cell study confirmed that 3.0 A dm^{-2} is the optimal c.d. for deposition of monolayer Zn-Ni alloy from the bath (optimized) given in Table 1. The Zn-Ni alloy coating developed at

3.0 A dm⁻² with ~8.0 wt.% Ni exhibited the least CR (14.46×10⁻² mm y⁻¹) compared to other coatings at other c.d.'s as reported in Table 2.

Table 1. Bath composition and operating parameters of the optimized bath.

Bath ingredients	Concentration, g L ⁻¹	Operating parameters
ZnCl ₂	27.2	Anode: Pure Zinc Cathode: Mild Steel pH 4.0 Temperature: 30 °C
NiCl ₂ x 6H ₂ O	94.9	
Boric acid	27.7	
NH ₄ Cl	100	
Gelatin	5.0	
Glycerol	2.5	

From the experimental data given in Table 2, it may be noted that the wt.% Ni in the electrodeposited Zn-Ni alloy at all c.d. are less than that in the bath (64.5 % Ni). Hence it may be inferred that the proposed bath follow anomalous type of codeposition, characteristic of all Zn-Fe group metal alloys, explained by Brenner [6]. Hence, Zn-Ni alloy coating at 3.0 A dm⁻², represented as (Zn-Ni)_{3.0/mono} has been taken as the optimal coating configuration for monolayer deposition from the proposed bath.

Table 2. Corrosion data for monolayer Zn-Ni alloy coatings developed at different c.d.'s.

<i>j</i> A dm ⁻²	Content of Ni Wt. %	-E ₀ V vs. SCE	<i>i</i> _{corr} μA cm ⁻²	CR × 10 ⁻² mm y ⁻¹
1.0	2.62	1.019	17.62	23.42
2.0	4.05	1.086	13.87	18.44
3.0	7.95	1.105	10.88	14.46
4.0	8.07	1.162	12.53	16.66

Optimization of cyclic cathode current densities (CCCD's) and number of layers in CMMA coatings

In the present work improving the corrosion resistance of monolayer Zn-Ni alloy by multilayer technique is guided by the following principles [23-25]:

- I. Periodic change in current density (c.d.) allows the growth of coatings having periodic change in its chemical composition.
- II. The corrosion resistance property of multilayer coatings or any functional property in general reaches its maximum value when thickness of the individual layers reaches optimal nanoscale.

The amplitude of compositional modulation diminishes rapidly when layer thicknesses below certain limit (about 50 nm).

Nanoscale multilayer coatings with alternate layers of alloys of different composition generally show unique properties than bulk materials when each individual layer thickness is below ~100 nm. Different layered combinations offer unique mechanical, optical, magnetic and electronic properties including improved good corrosion resistance. In all these cases, the properties of the multilayer coatings depend on two factors, namely the *composition* and *thickness* of the individual layers [26-28]. Hence by proper setting up of composition (by selection of cyclic current density, CCCD's) and thickness (by fixing the time for each layer deposition) of the individual layer it is

possible to optimize the coating configuration [29,30]. Hence multilayer coatings have been accomplished under different combination of CCCD's and individual layer thickness. The experimental procedure for optimization of coating configuration is explained below.

Multilayer coatings having 10 layers (arbitrarily chosen) have been developed at different CCCD's, namely at 1.0/3.0 and 2.0/4.0 A dm⁻², using same binary alloy bath. The coatings at different sets of CCCD's were developed in order to try different possible modulations in composition of individual layers, and their corrosion behaviours were studied, and corrosion data are reported in Table 3.

Table 3. Corrosion rates of CMMA Zn-Ni coatings having 10 layers at different CCCD's in comparison with (Zn-Ni)_{3.0/mono} developed from same bath.

CCCD's A dm ⁻²	-E ₀ V vs. SCE	i _{corr.} μA cm ⁻²	CR × 10 ⁻² mm y ⁻¹
(Zn-Ni) _{1.0/3.0/10}	1.085	8.416	11.18
(Zn-Ni) _{2.0/4.0/10}	1.108	6.606	8.78
(Zn-Ni) _{3.0/mono}	1.105	10.88	14.46

It may be noted that both (Zn-Ni)_{1.0/3.0/10} and (Zn-Ni)_{2.0/4.0/10} coatings exhibited less CR compared to (Zn-Ni)_{3.0/mono} coating. Hence, by choosing the above CCCD's, multilayer coatings with higher degree of layering, *i.e.* with 30, 60, 120, 300 and 600 layers have been developed by proper setting up of the power source. It may be noted the CR's decreased drastically with an increase in number of layers in both sets of CCCD's. It further indicates that improved corrosion property is not the unique property of the layer composition; instead, the combined effect of composition modulation and thickness of individual layers, or the number of layers. It should be noted that CR decreased only up to 300 layers and then started increasing, *i.e.* 600 layers as shown in Table 4.

Table 4. Effect of layering on corrosion behavior of CMMA (Zn-Ni)_{1.0/3.0} and (Zn-Ni)_{2.0/4.0} coating in comparison with monolayer (Zn-Ni)_{3.0/mono} deposited from same bath at 303K

Coating configuration	Number of layers	Average thickness of each layer, nm	E ₀ V vs. SCE	i _{corr} μA cm ⁻²	CR × 10 ⁻² mm y ⁻¹
(Zn-Ni) _{1.0/3.0}	10	1500	1.085	8.416	11.18
	30	750	1.037	7.125	9.47
	60	250	1.056	4.531	6.02
	120	125	1.067	2.357	3.13
	300	50	1.041	1.319	1.75
	600	25	1.050	3.577	4.75
(Zn-Ni) _{2.0/4.0}	10	1500	1.108	6.606	8.78
	30	750	1.085	4.989	6.63
	60	250	1.050	2.125	2.82
	120	125	1.007	1.056	1.40
	300	50	1.135	0.31	0.41
	600	25	1.036	1.975	2.61
(Zn-Ni) _{3.0/mono}	Monolayer	15000	1.128	10.78	14.33

Further, though decrease of CR was found in both sets of CCCD's, the CR corresponding to (Zn-Ni)_{2.0/4.0} at 300 layers is the least, it has been taken as the optimal configuration for peak

performance against corrosion, and is represented as $(\text{Zn-Ni})_{2.0/4.0/300}$. The CR found to increase at higher degree of layering, *i.e.* at 600 layers is due to shorter relaxation time for redistribution of metal ions at the diffusion layer, during plating. It should be noted that under optimal condition, the total thickness of CMMA $(\text{Zn-Ni})_{2.0/4.0/300}$ coating was found to be $\sim 15 \mu\text{m}$, calculated from thickness Tester (Coatmeasure Model M&C), verified by Faraday law. Then from the total thickness and number of layers allowed to form (300), it is predicted that the average thickness of each layer is 50 nm.

Thermal stability of the monolayer and multilayer coatings

Thickness and Hardness of the coatings

The thickness and hardness of coatings were found to be decreased on heat treatment in both $(\text{Zn-Ni})_{3.0/\text{mono}}$ and $(\text{Zn-Ni})_{2.0/4.0/300}$ coatings. In the case of $(\text{Zn-Ni})_{2.0/4.0/300}$ coatings the decrease may be attributed to the structural changes, evidenced by XRD study. The decrease is more pronounced in case of monolayer when compared to the multilayer Zn-Ni alloy coatings. The thickness of the coatings is directly related to the high tensile residual internal stresses, which result from the presence of Ni in the alloy [31]. The drop in the coating thickness with the temperature may be attributed to the iron enrichment caused by the formation of intermetallic Zn/Fe compounds due to the inter-diffusion at the coating/substrate interface. It was predicted that the iron enrichment in the interfacial region pushes nickel toward the surface [32]. The decrease of thickness and hardness with increase in temperature observed in case of $(\text{Zn-Ni})_{2.0/4.0/300}$ is shown, in comparison with that of $(\text{Zn-Ni})_{3.0/\text{mono}}$ coating in Table 5.

Table 5. Effect of temperature on thickness, hardness and corrosion behavior of CMMA $(\text{Zn-Ni})_{2.0/4.0/300}$ coatings, in comparison with monolayer $(\text{Zn-Ni})_{3.0/\text{mono}}$ deposited from same bath.

CCCD's A dm^{-2}	Treated temperature, $^{\circ}\text{C}$	Thickness, μm	Vicker hardness, V_{100}	$-E_{\text{corr}}$ V vs. SCE	i_{corr} $\mu\text{A cm}^{-2}$	$\text{CR} \times 10^{-2}$ mm y^{-1}
$(\text{Zn-Ni})_{2.0/4.0/300}$	30	18.9	212	1.003	0.31	0.41
	100	16.7	189	1.022	2.14	2.84
	200	14.3	183	1.024	2.18	2.89
	300	9.1	154	0.995	3.73	4.95
	400	5.4	139	0.865	4.52	6.00
$(\text{Zn-Ni})_{3.0/\text{mono}}$	30	17.8	202	1.128	10.78	14.33
	200	9.3	145	1.053	21.68	28.82
	400	4.8	119	1.070	26.53	35.27

Further, in the case of monolayer Zn-Ni coating the decrease of hardness may be attributed to the fact that the dislocation sources are active under the stress field (applied in the form of heat) [33]. The decrease in the residual stress is also reasoned to be responsible for decrease in hardness of the alloy coating with thermal treatment [34]. The CMMA coatings provide stress free environment, because the attractive forces tend to bridge the gap between successive layers. However, with heat treatment the interaction with the substrate increased, and hence stress developed.

Corrosion study

Cyclic polarization study

The corrosion resistance exhibited by Zn-Ni coatings (both monolayer and multilayer) can be better understood by Tafel polarization method as shown in Figure 2a, and corresponding

corrosion parameters are reported in Table 5. Cyclic polarization study over a potential range of -1.25V to -0.5V was studied and is shown in Figure 2b. The anodic current was made to move from negative to positive, and then reversed. Cyclic polarization curves shows that there is no much significance of the corrosion product formation with regard to the corrosion protection of the alloy. The corrosion current value was found to be always higher than that of forward scanning, indicating the dissolution of oxide film had occurred in the forward scanning and self-repairing occurred during the process of backward scanning. CMMA Zn-Ni coating with optimal configuration, $(\text{Zn-Ni})_{2.0/4.0/300}$ showing the least CR was opted for examining the thermal stability of the coatings. The CR of the Zn-Ni CMMA coating in 5% NaCl solution, before and after heat treatment of 100 °C represented as $(\text{Zn-Ni})_{2.0/4.0/300}$ and $(\text{Zn-Ni})_{2.0/4.0/300/100^\circ\text{C}}$, was found to be, respectively about 35 times and 5 times, respectively, more corrosion resistant than conventional $(\text{Zn-Ni})_{3.0/\text{mono}}$ alloy coating as shown in Figure 2b.

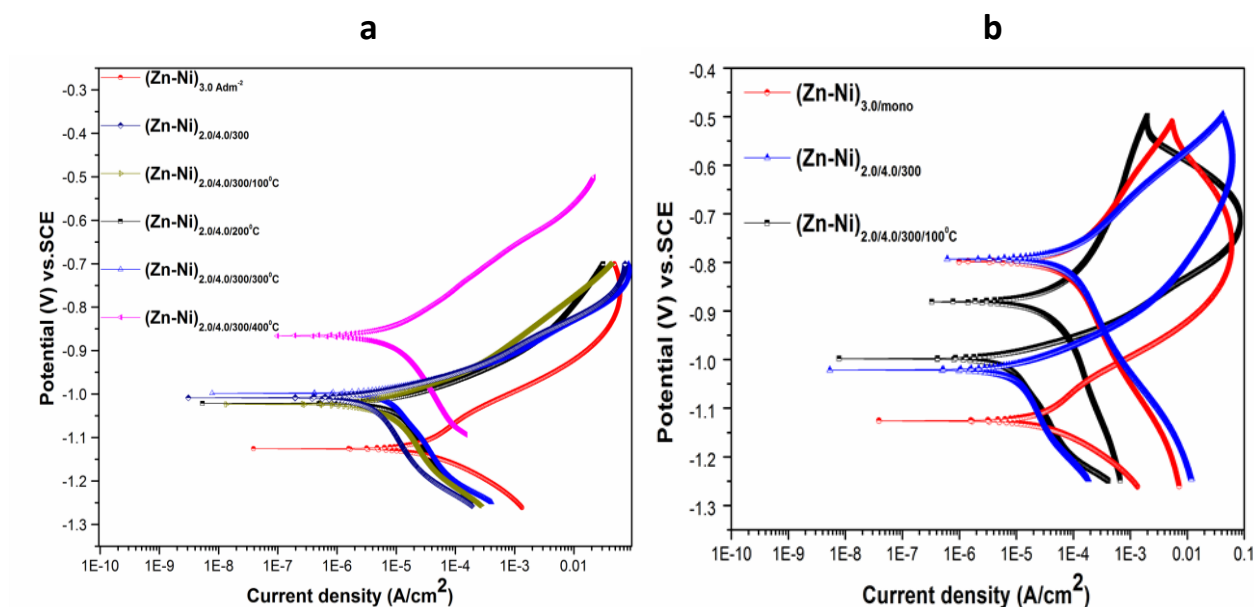


Figure 2. Polarization behavior of CMMA $(\text{Zn-Ni})_{2.0/4.0/300}$ Coatings: **a)** after treatment at different temperature **b)**, Cyclic polarization behavior of $(\text{Zn-Ni})_{3.0/\text{mono}}$ CMMA $(\text{Zn-Ni})_{2.0/4.0/300}$ and CMMA $(\text{Zn-Ni})_{2.0/4.0/300/100^\circ\text{C}}$.

Thus the corrosion resistance of multilayered Zn-Ni alloy coating has also decreased with heat treatment. However, the decrease in CR's were more significant in the case of multilayer Zn-Ni alloy coating compared to monolayer coating after heat treatment. It is due to the fact that the electroplated samples attained intrinsically different surfaces in terms of their electrochemical properties. However, increase in the CR's is not in proportion of the structural changes observed, as will be discussed with XRD analysis.

Electrochemical impedance spectroscopy study

The electrode process involved in double layer capacitance and corrosion behaviors can be better understood by electrochemical impedance spectroscopy (EIS) method. The small amplitude signals from the test specimen are considered in EIS method. The Nyquist plot is the type of the plot in which the data is plotted as imaginary impedance, Z_{img} vs. real impedance Z_{real} with the provision to distinguish the contribution of polarization resistance (R_p) versus solution resistance (R_s) [35]. EIS signals of Zn-Ni monolayer coating (at optimal c.d, i.e. 3.0 A dm^{-2}) compared with the $(\text{Zn-Ni})_{2.0/4.0/300}$ coating before and after heat treatment (at different temperatures) is shown on

Figure 3. Progressive decrease of polarization resistance of CMMA coatings with annealing temperature supports the reduced corrosion resistance, may be due to diffusion of layers. However, corrosion rate of monolayer coatings are more than multilayer coatings under all degree of layering.

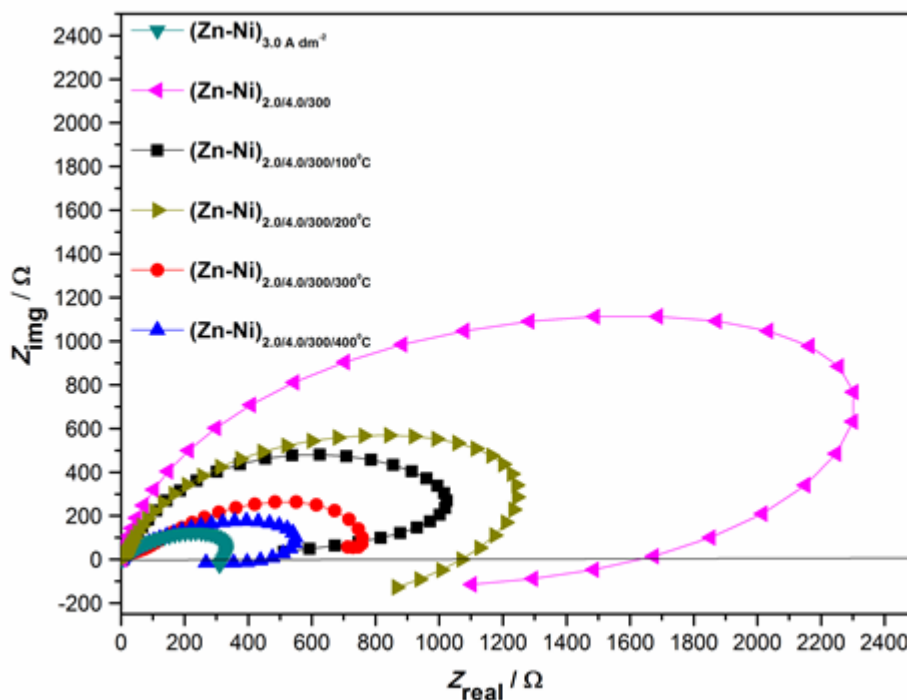


Figure 3. Electrochemical impedance response (Real vs. Imaginary reactance values) displayed by CMMA (Zn-Ni)_{2.0/4.0/300} after heat treatment at 4 different set temperatures.

It may be noted that all the coatings exhibits one capacitive loop. However, at low frequency limit the capacitive behaviour of the double layer tends to exhibit the inductive character, indicated by decrease of both Z_{real} and Z_{img} . The gradual decrease in the diameter of semicircle indicates that the polarization resistance, R_p decreases with increase in temperature as shown in Figure 3. The (Zn-Ni)_{2.0/4.0/300} coating showed maximum impedance, due to accumulation of corrosion products at the electrode surface acting as barrier. The negative value of imaginary impedance, Z_{img} at lower frequencies observed in coatings treated for higher temperatures are attributed to the inductance behaviour caused by the change in corrosion potential at the interface [36,37]. However, the radii of both capacitive loop and inductive character decreased progressively with raise in temperature.

Surface morphology

Figure 4 displays the SEM image for surface morphology of (Zn-Ni)_{2.0/4.0/300} alloy coatings after heat treatment at different temperatures. It may be noted that the surface non-homogeneity increased with an increase of treatment temperature. However, Zn-Ni alloy coatings are found to adhere onto the substrate as fine particles with compact arrangement. The increased compactness with the heat treatment was also predicted to be main reason for good appearance and high hardness [38].

The cross sectional view of CMMA (Zn-Ni)_{2.0/4.0/10} coating before and after heat treatment (100 °C) is shown in Figure 5. It may be noted that distinctly visible alloy layers (Figure 5a) become

fused (Figure 5b) due to diffusion of layers upon heat treatment. Thus thermal treatment of electrodeposited multilayer Zn-Ni alloy coatings leads to both structural and behavioral changes.

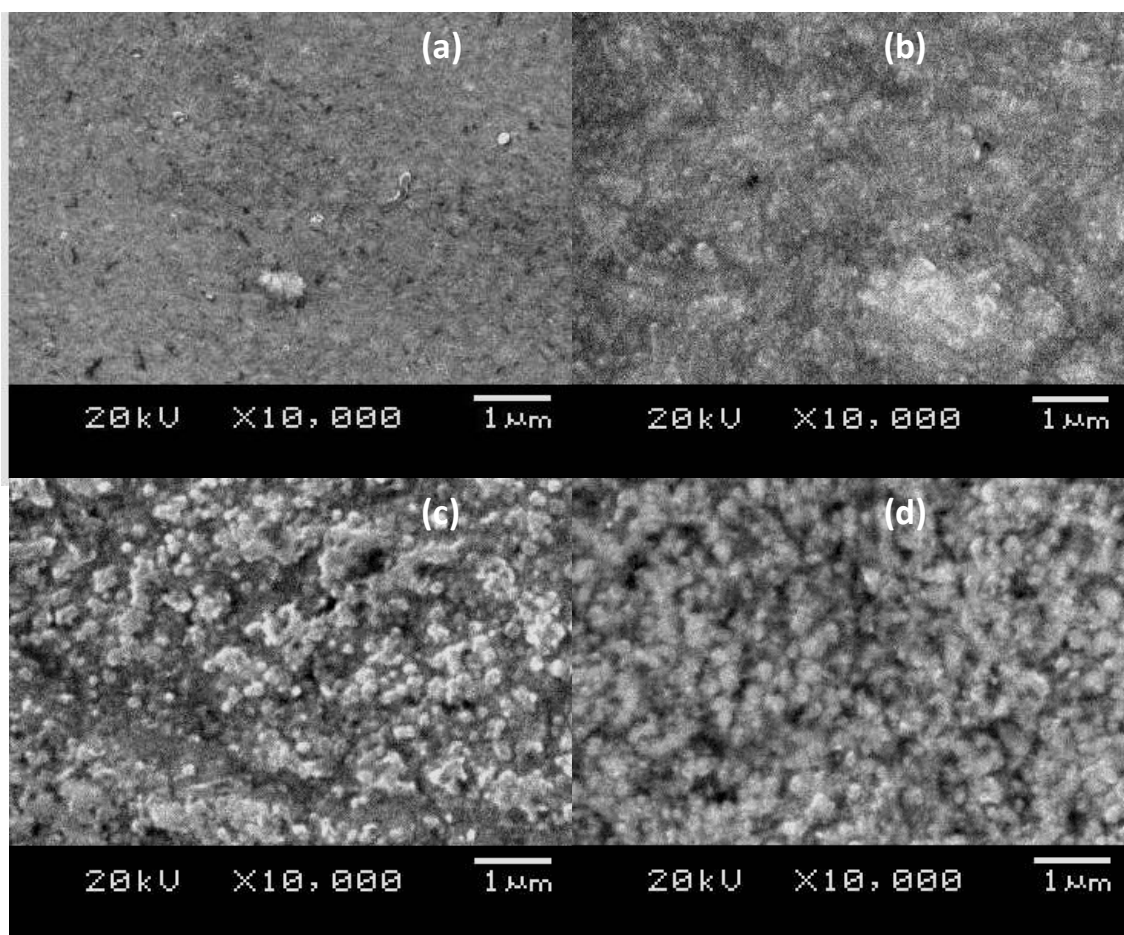


Figure 4. SEM images of CMMA (Zn-Ni)_{2.0/4.0/300} coatings after treatment at different temperatures: (a) 100°C (b) 200°C (c) 300°C and (d) 400°C.

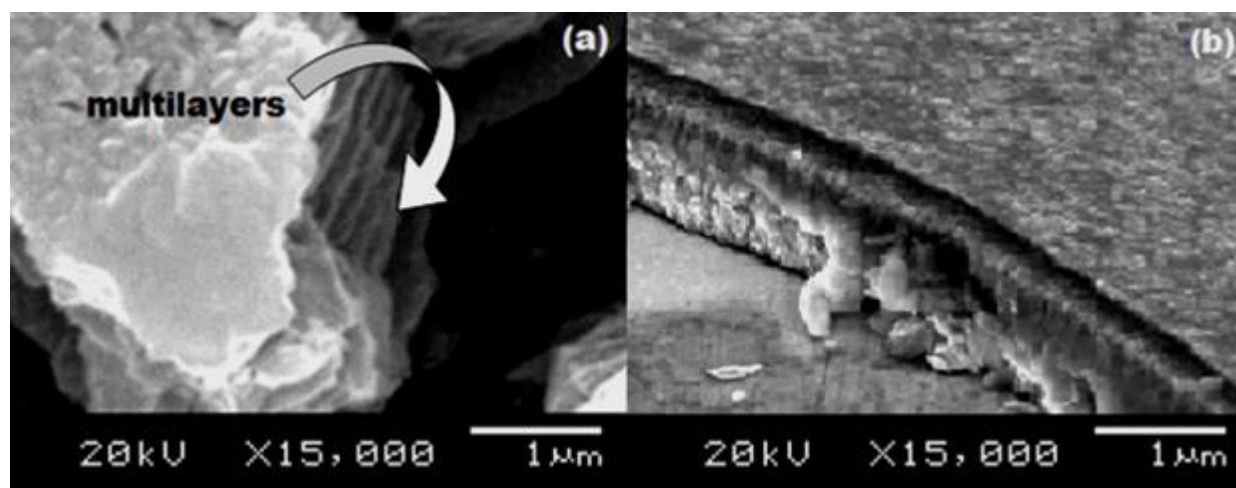


Figure 5. SEM images across the cross section of CMMA (Zn-Ni)_{2.0/4.0/10} coatings before heat treatment (a), and after heat treatment at 200°C (b).

XRD study

The XRD patterns of (Zn-Ni)_{3.0/mono} and (Zn-Ni)_{2.0/4.0/300} alloy coating after heat treatment, deposited from same bath is given in Figure 6 and 7 respectively. Variation in the surface morphology of the monolayer coatings after heat treatment is supported by the variation in XRD

peaks. It has been reported that the phases obtained by the Zn-Ni coatings up to 13 % nickel do not correspond to that reported on the thermodynamic phase diagram [39]. It may be noted that the reflection corresponding to Zn(101), γ -phase ($\text{Ni}_5\text{Zn}_{21}$), Zn(103) phases and $\text{Ni}_3\text{Zn}_{22}$ (335) as well was observed in monolayer coating deposited at optimal c.d. *i.e.*, 3.0 A dm^{-2} . However, upon heat treatment there was hardly any difference in the phases observed in the $(\text{Zn-Ni})_{3.0/\text{mono}}$ alloy coatings before and after heat treatment up to 200°C . However, at temperatures higher than 200°C additional phases were observed corresponding to the intermetallic Zn/Fe compound (Figure 6). The formation of this phase occurs due to inter diffusion in the interface region between the Zn-Ni alloy and the steel substrate. ZnO phase formation at temperatures higher than 200°C was attributed to the metal contact with the ambient oxygen. The X-ray diffraction line broadening at temperatures higher than 200°C may be related to the increase in the corrosion current value, which is reported to be caused by the lattice strains [40].

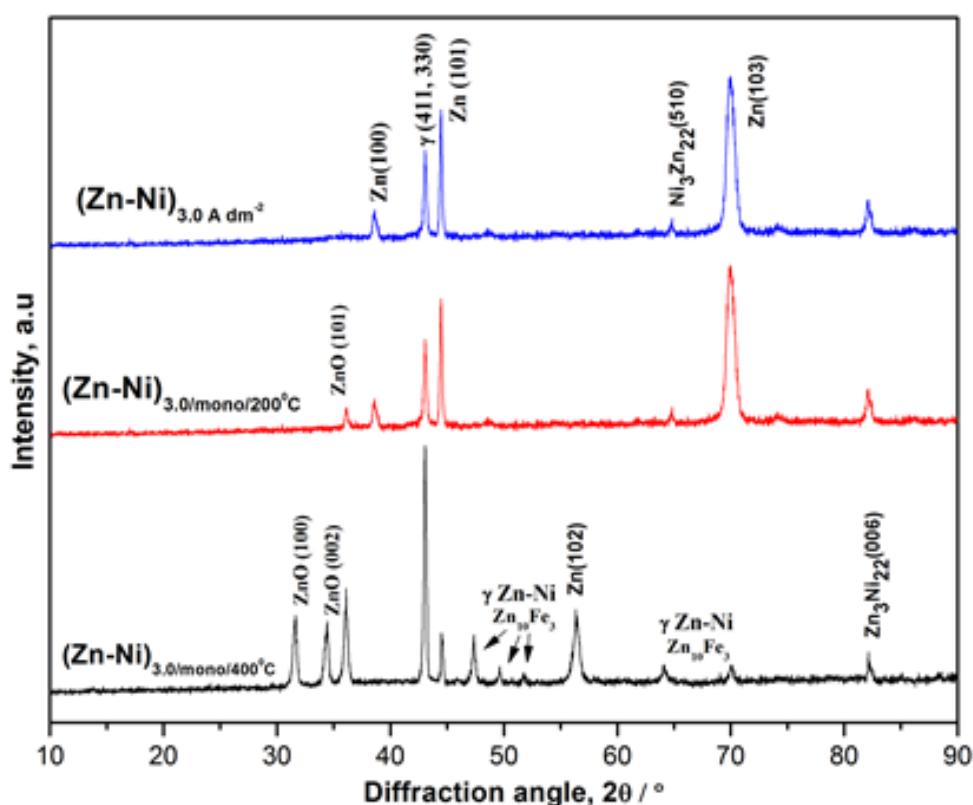


Figure 6. XRD patterns of the $(\text{Zn-Ni})_{3.0/\text{mono}}$ coatings after heat treatment at different temperatures (200°C and 400°C) deposited from the same bath.

The reflection corresponding to Zn(101), γ -phase ($\text{Ni}_5\text{Zn}_{21}$) and $\text{Ni}_3\text{Zn}_{22}$ (510) was highly suppressed in the case of $(\text{Zn-Ni})_{2.0/4.0/300}$ coating on heat treatment at 4 different set temperatures. However at temperatures higher than 300°C , the coating has shown weak signal corresponding to Zn(100), Zn(102) and γ Zn-Ni phases, although Zn(103) phase completely disappeared. The least CR exhibited by $(\text{Zn-Ni})_{2.0/4.0/300/100}$ was attributed to the ratio of the phase structure corresponding to Zn(103) and weak signals corresponding to γ -phase of Zn (411, 330), Zn(101) and $\text{Zn}_3\text{Ni}_{22}$ (006) phase. The comparison between the XRD signals of the Zn-Ni monolayer and CMMA coating on post-heat treatment reveals the fact that the exhibition of lesser CR of the Zn-Ni CMMA coating upon heat treatment to that of the Zn-Ni monolayer coating deposited at optimal c.d. *i.e.*, 3.0 A dm^{-2} , was attributed to the diffusion of the layered structure and formation of different phase structure ratio as shown on Figure 6 and Figure 7.

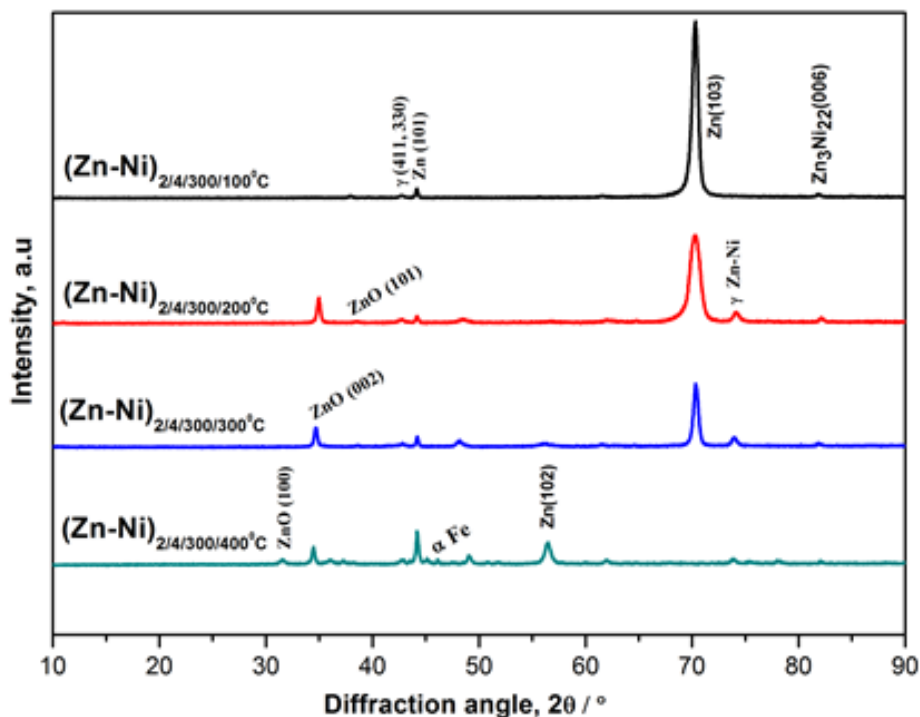


Figure 7. XRD patterns of the CMMA (Zn-Ni)_{2.0/4.0/300} coatings after heat treatment at different temperature (100°C, 200°C, 300°C and 400°C), deposited from the same bath.

Conclusions

Based on the experimental investigation on development and characterization of CMMA Zn-Ni alloy coatings on mild steel following observations were made as conclusions:

1. The coating configuration in terms CCCD's and number of layers have been optimized for deposition of the most corrosion resistant coatings from acid chloride bath using glycerol and gelatin as additives.
2. The decrease in thickness and hardness of both monolayer and multilayer coatings due to heat treatment were due to the active dislocation sources and decrease in the residual stress.
3. Progressive decrease of polarization resistance of CMMA coatings with annealing temperature supports the reduced corrosion resistance, may be due to diffusion of layers. However, corrosion rate of monolayer coatings are more than multilayer coatings under all degree of layering.
4. The corrosion resistance of multilayer coatings increased only up to certain number of layers and then decreased due to interlayer diffusion.
5. Thermal treatment of electrodeposited (both monolayer and multilayer) Zn-Ni alloy coatings led to significant structural change of the alloy, supported by SEM and XRD study.
6. A small increase of corrosion rates of Zn-Ni alloy due to annealing is related to the formation of a more ordered lattice of the alloy.
7. However, the increase of corrosion rates, due to annealing is not in proportion of the structural changes of the alloy occurred.
8. The corrosion resistance of both multilayered and monolayer coatings decreases with heat treatment. However, it is more pronounced in case of monolayer coatings. It is due to the fact that the electroplated samples attained intrinsically different interfacial structures.

9. The structural changes due to heat treatment of monolayer Zn-Ni alloy coatings continue to exist even in multilayer coatings. Further, the structural changes in alloy composition (both monolayer and multilayer) are found to be a function of annealing temperatures.

Acknowledgement: Mr. Vaishaka R.Rao acknowledges National Institute of Technology Karnataka (NITK), Surathkal for financial support in the form of Institute Fellowship.

References

- [1] G. Injeti, B. Leo, *Adv. Mater.* **9** (2008) 1–11.
- [2] P. Ganesan, S. P. Kumaraguru, B. N. Popov, *Surf. Coat. Technol.* **20** (2007) 7896–7904.
- [3] V. Thangaraj, N. Eliaz, A. C. Hegde, *J. Appl. Electrochem.* **39** (2009) 339–345.
- [4] S. Yogesha, A. C. Hegde, *J. Mater. Process. Technol.* **211** (2011) 1409-1415.
- [5] W. Blum, *Trans. Am. Electrochem Soc.* **40** (1921) 307-320.
- [6] A. Brenner, *Electrodeposition of Alloy*, Academic Press., New York, p. 194.
- [7] D. Tench, J. White, Tensile, *J. Electrochem Soc.* **138** (1991) 3757-58.
- [8] Zhongda Wu, L. Fedrizzi, P.L. Bonora, *Surf. Coat. Technol.* **85** (1996) 170-174.
- [9] R. Ramanauskas, I. Muleshkova, L. Maldonado, P. Dobrovolskis, *Corros. Sci.* **40** (1998) 401-410.
- [10] M. Gavrilu, J.P. Millet, H. Mazille, D. Marchandise, J.M. Cuntz, *Surf. Coat. Technol.* **123** (2000) 164–172.
- [11] J.B. Bajat, Z. Kacarevic-Popovic, V.B. Miskovic-Stankovic, M.D. Maksimovic, *Prog. Org. Coat.* **39** (2000) 127–135.
- [12] R. Fratesi, G. Roventi, *Surf. Coat. Technol.* **82** (1996) 158-164.
- [13] Jing-yin Fei, G.D. Wilcox, *Surf. Coat. Technol.* **200** (2006) 3533 – 3539.
- [14] M. Rahsepar, M.E. Bahrololoom, *Corros. Sci.* **51** (2009) 2537–2543.
- [15] K. Venkatakrishna, A. C. Hegde, *J. Appl. Electrochem.* **40** (2010) 2051–2059.
- [16] A. Maciej, G. Nawrat, W. Simka, J. Piotrowski, *Mater. Chem. Phys.* **132** (2012) 1095–1102.
- [17] Y. Liao, D.R. Gabe, G.D. Wilcox, *Plat. Surf. Finish.* **85** (1998) 88-91.
- [18] J.-L. Chen, J.-H. Liu, S.-M. Li, M. Yu, *Mater. Corros.* **63** (2012) 607-613.
- [19] S. Yogesha, R.S. Bhat, K. Venkatakrishna, G. P. Pavithra, Y. Ullal, A.C. Hegde, *Synth. React. Inorg. Met.-Org. Chem.* **41** (2011) 65-71.
- [20] R.S. Bhat, K.R. Udupa, A.C. Hegde, *Trans. Inst. Met. Finish.* **89** (2011) 268-274.
- [21] V. Thangaraj, K. Ravishankar, A.C. Hegde, *Chin. J. Chem.* **26** (2008) 2285-2291.
- [22] R. S. Bhat, K. U. Bhat, A. C. Hegde, *Prot. Met. Phys. Chem. Surf.* **47** (2011) 645-653.
- [23] F. Jing-yin, L. Guo-zheng, X. Wen-li, W. Wei-kang, *J. Iron. Steel Res. Int.* **13** (2006) p. 61-67.
- [24] R.S. Bhat, A.C. Hegde, *Surf. Eng. Appl. Electrochem.* **47** (2011) 112-119.
- [25] B.N. Popova, S. Kumaragurua, P. Ganesana, *J. Electrochem Soc.* **1** (2006) 87-96.
- [26] K.K. Chattopadhyay, A.N. Banerjee, *Introduction to Nanoscience and Technology*, Connaught Circus, New Delhi, India, 2009, p. 155.
- [27] V.K. Varadan, A.S. Pillai, D. Mukherji, M. Dwivedi, L. Chen, *Nanoscience and Nanotechnology in Engineering*, World Scientific Publishing Co. Pvt. Ltd. Singapore, 2010, p. 170.
- [28] D.R. Baer, P.E. Burrows, A.A. El-Azab, *Prog. Org. Coat.* **47** (2003) 342-356.
- [29] K. Venkatakrishna, A. C. Hegde, *Mater. Manuf. Processes.* **26** (2011) 29–36.
- [30] S. Yogesha, K. Venkatakrishna, A. C. Hegde, *Anti-Corros. Methods Mater.* **58** (2011) 84-89.
- [31] H.J.C. Voorwald, I.M. Miguel, M.P. Peres, M.O.H. Cioffi, *J. Mater. Eng. Perform.* **14** (2005), 249-257.
- [32] J. Kondratiuk, P. Kuhn, E. Labrenz, C. Bischoff, *Surf. Coat. Technol.* **205** (2011) 4141-4153.
- [33] L. P. Bicelli, B. Bozzini, C. Mele, L. D'Urzo, *Int. J. Electrochem. Sci.* **3** (2008) 356 – 408.
- [34] B.K. Prasad, *Mater. Sci. Eng.* **A277** (2000) 95-101.

- [35] V. M. Huang, Shao-Ling Wu, M. E. Orazem, N. Pebere, B. Tribollet, V. Vivier, *Electrochim. Acta.* **56** (2011) 8048-8057.
- [36] U.C. Nwaogu, C. Blawert, N. Scharnagl, W. Dietzel, K.U. Kainer, *Corros. Sci.* **52** (2010) 2143–2154.
- [37] R. Ghosh, D.D.N. Singh, *Surf. Coat. Technol.* **201** (2007) 7346– 7359.
- [38] M. Pushpavanam, S.R. Natarajan, K. Balakrishan, L.R. Sharma, *J. Appl. Electrochem.* **21** (1991) 642-645.
- [39] C. Bories, J.P. Bonino, A. Rousset, *J. Appl. Electrochem.* **29** (1999) 1045-1051.
- [40] R. Ramanauskas, R. Juskenas, A. Kalinichenko, *J. Solid State Electrochem.* **8** (2004) 416-421.